Mechanics of Advanced Composite Structures 5 (2018) 75-81

Semnan University

Mechanics of Advanced Composite Structures

Journal homepage: http://MACS.journals.semnan.ac.ir

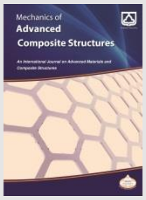

Evaluation of hardness and wear resistance of nano-sized titanium-carbide-reinforced commercially cast aluminum alloy matrices

M. Mafi[a] , B. Ghasemi[a,*], O. Mirzaee[a]

[a] *Faculty of Materials and Metallurgical Engineering, Semnan University, Semnan, Iran*

PAPER INFO

Paper history:
Received 2016-11-29
Revised 2017-10-31
Accepted 2018-01-01

Keywords:
Metal–matrix composites
Mechanical testing
Electron microscopy
Casting

ABSTRACT

Production of aluminum matrix composites is widespread because these material provide enhanced mechanical properties compared to aluminum. One the most important parameters of metal matrix composite production is uniform distribution of reinforcing nanoparticles in matrices using the stir-casting method. Second is ensuring high wettability, which is determined by evaluating the properties of materials on a nano-scale. In this study, aluminum composites were reinforced with titanium carbide nanoparticles coated with aluminum to increase wettability. Particles were prepared and added to a molten aluminum alloy. After stirring the particle mixture as a variable parameter, casting was conducted in a sand mold. To evaluate the mechanical properties of the composite, the Brinell test was used to determine hardness and the pin-on-disk test was used to measure wear rate and the friction coefficient. The results showed that the hardness of the composite increased from 84 BHN to 134 BHN as nanoparticles were added to the alloy. Additionally, as stirring time increased, weight loss decreased with respect to the base alloy, while the coefficient of friction increased.

1. Introduction

Aluminum matrix composites have been significantly utilized in the automotive, military, and aerospace industries due to properties such as high special strength, resistance to abrasion, low thermal conduction coefficients, and high oxidation resistance. Reinforcement of such composites can be accomplished using particles, continuous fibers, short fibers, and whiskers; however, particle reinforcement is most common due to its simple production process and resulting isotropic properties of the composite [1]. Most commonly, ceramic particles are used to reinforce aluminum matrix composites, including Si, Al_2O_3 and ZrO_2, TiC, and B_4C, which can be utilized on nano and micron scales [1–3]. Among ceramic particles, titanium carbide (TiC) is often used to reinforce aluminum matrix composites because it has a high melting point (3,160°C), adequate thermal stability, high hardness, resistance to abrasion, high impact resistance, a high neutron-absorption cross section, and adequate reduction potential (to 25 mV).

Metal matrix composites are advanced materials with advantages over common metals and alloys, such as higher strength-to-weight ratios and higher resistance to abrasion. These benefits are created during production of composites and are valuable for an extensive range of applications [3–6]. Composites produced by stir casting are affordable and allow components to be produced in various shapes and compositions. The primary limitation of composites is the wettability of ceramic particles, which affects

---

[*] Corresponding author. Tel.: +98 9122055283 ; Fax: +98-23 33654119
E-mail address: bghasemi@ Semnan.ac.ir

DOI: 10.22075/MACS.2018.1770.1091

proper distribution of secondary phases in the matrix. The stir-casting process is simple, affordable, and flexible and can be used with many materials; however, limitations include low wettability, separation, agglomeration, and inconsistent distribution of reinforcement particles in a matrix [7–9].

2. Experimental procedure

Aluminum alloy (LM2; Table 1) was used as the matrix material in this study, with TiC used as the reinforcement material for the composite matrix. The TiC was obtained as semi-spherical, 60 nm particles with a purity of 99%, and aluminum and copper powders, with an average particle size of 50 µm, were used as components of the reinforcement powders. These powders were mixed at a mass ratio of Al/TiC = 1 and Cu/TiC = 1 and milled in a wet planetary mill for 2 h.

To fabricate the composites, 500 g of LM2 was placed in a resistance furnace, equipped with a graphite stirring system. To produce a TiC/2 vol% nano-TiC metal matrix composite, an appropriate amount of mixed powders was wrapped in aluminum foil and added to the molten alloy during stirring, which was carried out at a constant rate of 450 rpm for 4, 6, and 12 min at 850°C. The composite slurry was poured into a cast-iron, cylindrical mold with a 14 mm outer diameter and a height of 140 mm (Fig. 1). The as-cast specimens were heat-treated (T6) using the following schedule: 8 h at 495°C, followed by 2 h at 520°C before water quenching (40°C) and artificially aging for 8 h at 180°C [10].

To study the microstructure of the specimens, samples were cut and prepared by grinding with 400–2,500 grit paper, polishing with 0.3 lm alumina paste, and etching with a Keller's reagent. Microscopic examinations of the composites were carried out using a scanning electron microscope (SEM; CAMSCAN-MV 2300), and an image analysis was performed to determine the grain size of the samples.

The porosity percentage of the composites was determined by comparing the measured density to the theoretical density. To study hardness fluctuations in the longitudinal parts of the cylindrical composite (i.e., the hardness profile), Brinell hardness values were obtained for the samples by measuring the samples using a ball with a 5 mm diameter under a load of 125 kg (Ernst-Twin, Model), according to the ASTM E10–12 standard. Each hardness value was an average of at least five random hardness readings. The wear test was carried out under dry condition on a pin-on-disc apparatus, according to ASTM G99–95A, and dry-sliding wear tests were conducted using a conventional pin-on-disc testing machine to appraise room temperature wear behavior of the Al-TiC composites against a DIN 100Cr6 steel disk with a hardness of 62 HRC. The pins, 5 mm x 15 mm, were in conformal contact with the steel disk, which rotated at a speed of 180 rpm. The test was carried out for a constant distance of 500 m under a normal load of 7 N, and the wear properties were measured in terms of material weight loss to 0.1 mg of resolution. For the sake of accuracy, three samples were prepared and tested, and the mean value was reported. The worn debris were analyzed using an SEM equipped with an energy dispersing X-ray analysis accessory [11–13].

3. Results and discussion

Figure 2 shows nanoparticles on the surface of the TiC–Cu mixed powders covered with fine nano-TiC particles. Using Bouvard's model, fine reinforcement particles were shown to cover the surface of the coarse metallic powders, and a metallic and ceramic powder mixture was added to the molten aluminum [14].

Figure 3 shows an SEM micrograph of the composites, while Figure 3a shows the uniform distribution and well-bonded nano-TiC particles in the TiC–Al reinforced composite, which was stirred for 12 min. Figure 3b illustrates the distribution of the nanoparticles in the same sample, reinforced by TiC–Cu mixed powders. These samples were selected from the middle section (7 cm) of the cylindrical specimen.

Table 1. Chemical composition of LM2 (wt%)

Element	Si	Fe	Cu	Mg	Ni	Zn	Pb	Sn
%	9–11	1	0.7–2.5	0.3	0.5	02	0.3	0.2

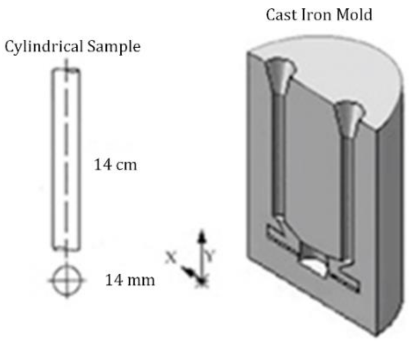

Figure 1. The fabricated cylindrical specimen

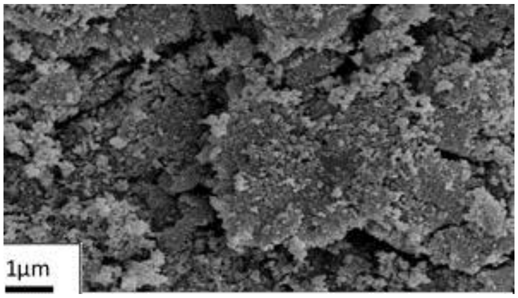

Figure 2. SEM image of the surface of TiC–Cu mixed powders

Figures 3c and 3d show the agglomerated particles in the samples selected from the bottom edge of the cylindrical specimens (0 cm) in TiC–Al and TiC–Cu reinforced composites, respectively. Microstructural characterization showed that the number and size of agglomerated particles varied in position in the sample, throughout the length of the cylindrical composite, but increased in the samples selected from the bottom edges of the cylinders. This can be explained according to Stokes' Law [15–16].

The Energy-dispersive X-ray spectroscopy (EDS) analysis of the TiC–Cu reinforced sample showed that it contained 2 wt% of Cu. Factors such as particle absorption by gas bubbles and particle floating or sinking in molten alloy affected particle distribution in the matrix, in addition to the parameters of the stirring process, such as stirring speed, stirring time, and the position of the stirrer in the molten composite, which affected uniform distribution of particles in different parts of the composite. Thus, the stirring process was modified according to previous studies [17–18]. To evaluate the effect of the milling process and stirring time on particle distribution in different parts of the composites, hardness profiles were compiled, and to evaluate hardness fluctuations, the specimens were cut into equal sections in a longitudinal direction, and the Brinell hardness test was performed.

Figure 4 shows hardness fluctuations in the heat-treated samples. As shown in the hardness diagram, hardness increased when nano-TiC powder was added, which caused grain refining and prevented dislocation movements. Since TiC is harder than aluminum, adding TiC particles to LM2 produced a significantly harder composite compared to the original alloy. The hardest sample resulted from the composite produced after 6 min of stirring. Figure 4 also shows hardness fluctuation for aluminum and copper particles coated with TiC mixed for 4 and 6 min. This nanocomposite was also harder than the original alloy [19–20].

Weight loss and wear rate variations in the composites based on stirring time are shown in Figure 5. Adding low amounts of Tic enhanced the abrasive properties of the LM2. In the composites, material removal was delayed because TiC particles accumulated on the surface of the samples after the alloy had been removed during abrasion. These hard particles effectively resisted the micro-cutting action of the abrasives [21–22] due to the higher hardness levels of TiC particles compared to the LM2 matrix. The wear rate of the composites were almost when stirring time was reduced to less than 6 min for the TiC–Cu reinforced composites. Based on the parameters that affected wear resistance, porosity content was the dominant factor affecting the wear properties of various samples in the present study.

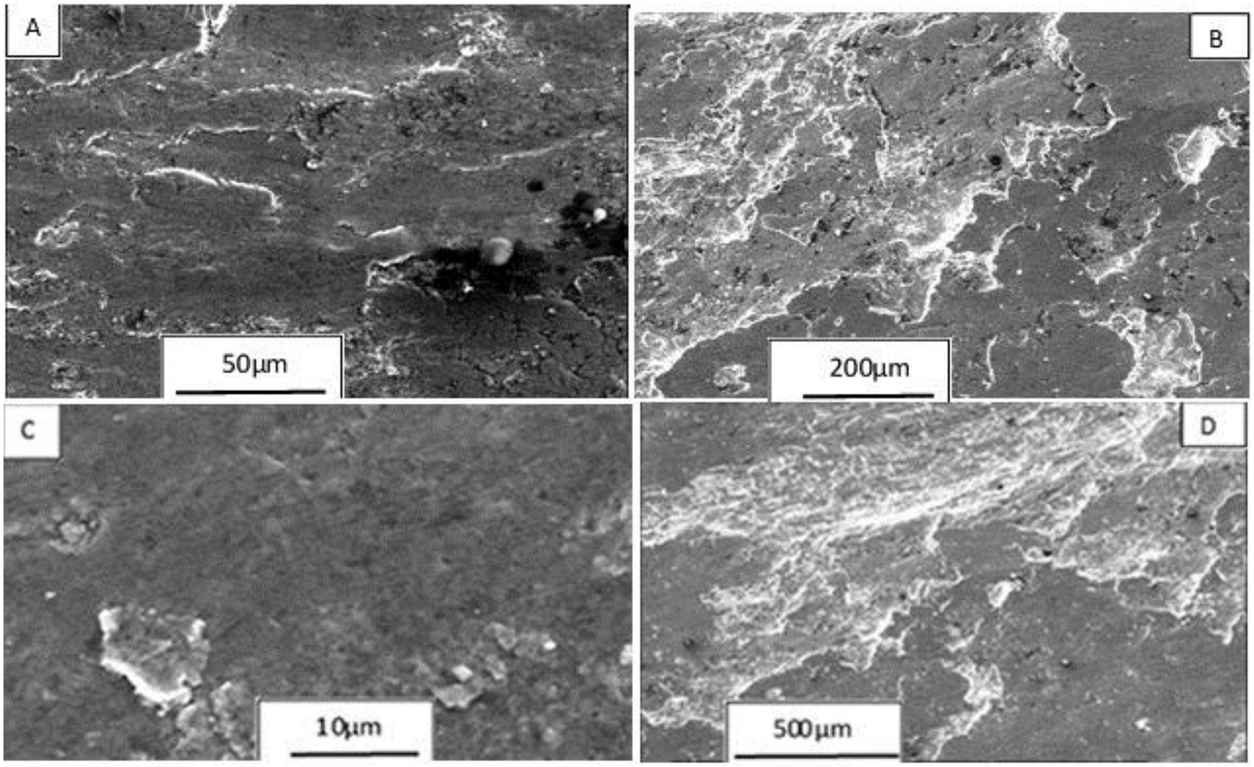

Figure 3. SEM images of nanocomposites: (a) uniformly distributed nano-TiC particles in TiC–Al, (b) TiC–Cu reinforced composites, (c) agglomerated nano-TiC particles in TiC–Al, and (d) TiC–Cu reinforced composites

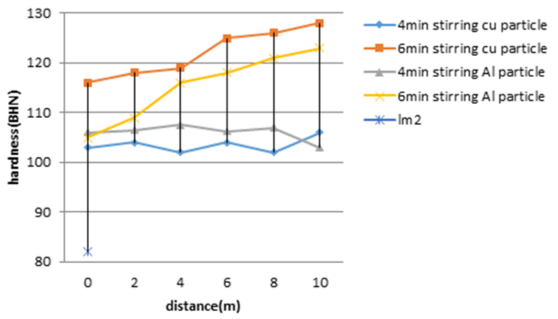

Figure 4. Hardness fluctuations in various composites stirred for 4 and 6 min

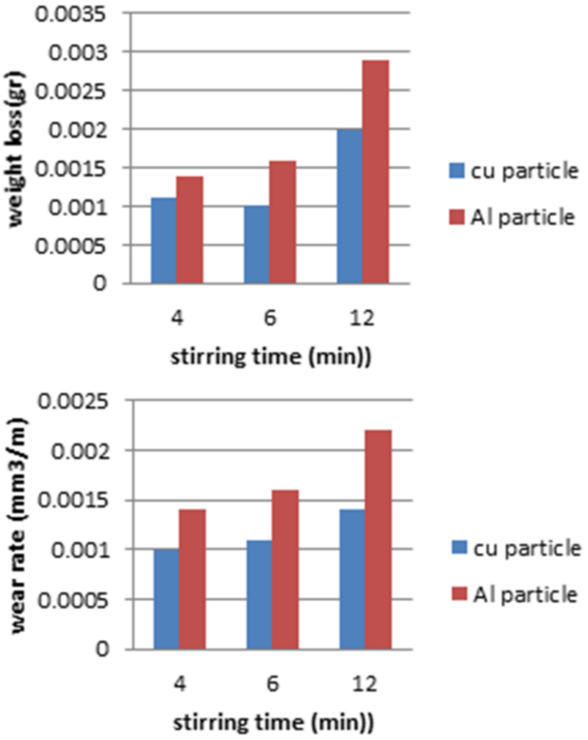

Figure 5. Variations in the weight loss and wear rate of composites with stirring time and a constant sliding distance of 600 m

Figure 6 presents variations in wear rate with the hardness of the composites at different stirring durations. A comparison of hardness shows a significant difference between the highest and lowest values of hardness for TiC–Al and TiC–Cu reinforced composites. The results indicate that the hardness of TiC–Al reinforced samples decreased after 4 min of stirring but that the hardness of TiC–Cu reinforced samples decreased after 6 min of stirring. Despite this, hardness was localized to deformations in the material, which was not attributed to porosity. However, porosity was a major factor affecting hardness of the composites, and an increase in porosity was accompanied by a reduction in wear rate, although this was not consistent with changes in porosity, especially in the TiC–Cu reinforced samples.

These results suggest that, although the main controlling factor was porosity, other parameters influenced samples' wear behavior. The enhanced mechanical properties of TiC–Cu reinforced samples compared to those of the TiC–Al reinforced composites can be attributed to the strengthening effect of copper on the aluminum matrix, which was improved by the T6 heat treatment. The application of a two-stage solution heat treatment to cast aluminum alloys reduced and refined the as-cast copper-rich phase of the LM2 alloy, creating better homogenization of the aluminum matrix prior to aging. Second-stage solution treatment temperatures higher than 520°C are not recommended because this causes incipient melting of the copper eutectic phase, resulting in degradation of mechanical properties [23].

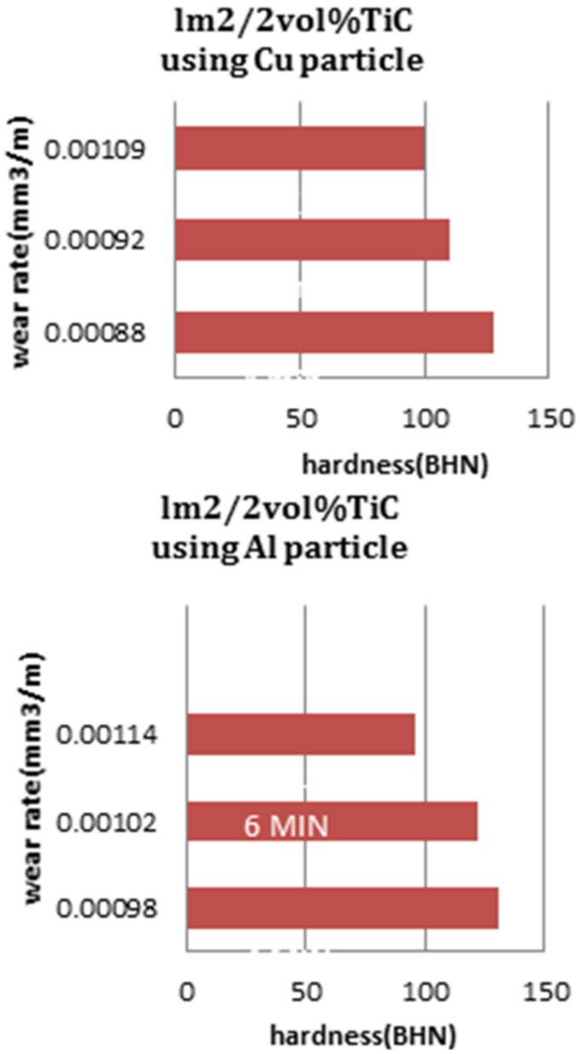

Figure 6. Variations in wear rate as a function of hardness and stirring time

Researchers have reported that the wettability behavior of TiC plates coated with copper using the electroless method improved immersion in molten aluminum. The wettability angle was reduced from 115.2 at the interface of the molten aluminum on the uncoated TiC plate to a minimum contact angel of 12.6 at the interface of the molten aluminum on the copper coated TiC plate, based on a sessile drop test at 800°C [24]. This laboratory experiment showed that the behavior of copper particles affects particle distribution in molten alloys and the mechanical properties of samples. Furthermore, copper increases the fluidity of aluminum alloys [25].

According to the microstructures of the composites, particle distribution in the TiC–Cu reinforced samples was more consistent than in the TiC–Al reinforced samples; thus, better mechanical performance in the TiC–Cu reinforced samples could be related to the effects of copper powders on particle distribution and age hardening. To evaluate the fluctuation of wear resistance among the composites, disc samples were selected from the top (14 cm), bottom (0 cm), and middle (7 cm) sections of the cylindrical samples and tested under the same conditions.

Abrasion rate varied among sample. Figure 7 shows the abrasion rate of the longitudinal cylindrical samples mixed for 4 and 12 min. The selected samples were from the topmost, middle, and the lowest part of the cylinder (i.e., the edge), which endured the highest gravity force. The results indicated that the sample mixed for 12 min had a higher abrasion rate compared to the sample mixed for 4 min due to gas trapped during mixing and porosity. Gas entrapment during particle incorporation or mixing leads to poor distribution of particles, which attach to gas bubble; thus, the higher porosity of the samples stirred for 12 min affected particle distribution. This, combined with the effects of higher stirring durations on particle distribution (i.e., shear forces and harmful entrapped gas), caused more uniform particle dispersion in the samples stirred for 12 min compared to the sample stirred for 4 min. This is also responsible for increased wear rates in the samples stirred for longer durations. Although samples were quickly solidified, gravity did not affect the suspension behavior of nanoparticles; rather, the amount of nanoparticles linearly increased from the top to the bottom of the cylinders, which is a process that cannot be easily measured by ordinary methods. Nanoparticle suspension or sinking was significantly affected by gravitational force, based on Stocks' law.

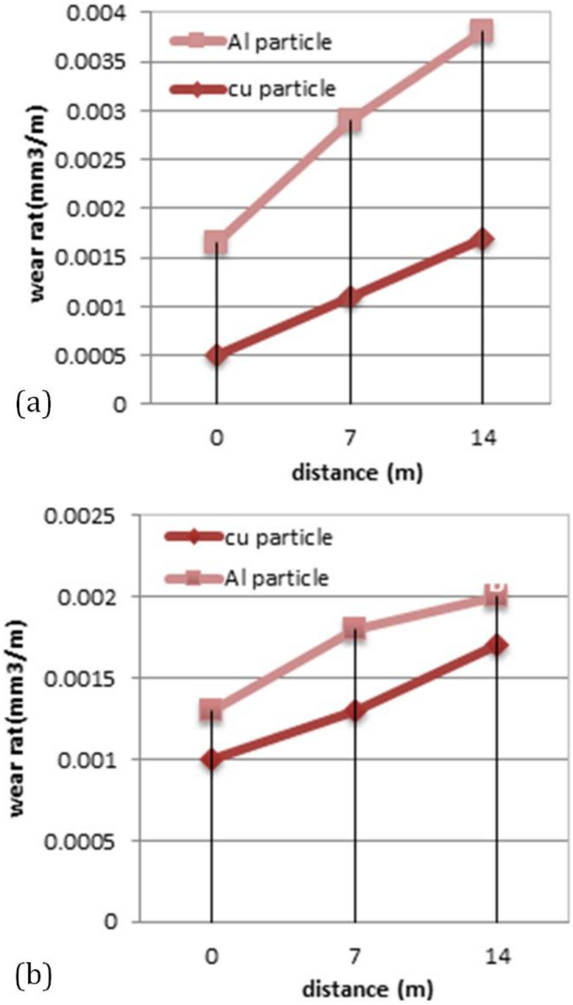

Figure 7. Fluctuation of wear rates among composites (a) stirred for 4 min and (b) 12 min

The wear debris morphology and EDS analysis results for the non-reinforced alloy and the composites are shown in Figure 8. Wear debris shows a flake-like morphology for both the non-reinforced and reinforced samples; a flaky morphology indicates delamination.

4. Conclusion

In the current study, nano-TiC particles were separately milled with aluminum and copper powders and incorporated into an LM2 alloy using the stir-casting method to fabricate LM2/2 vol% nano-TiC composites. SEM micrographs indicated that various mixed powders affected the quality of particle distribution in the matrix, which was also affected by stirring durations. Agglomerated particles were observed in the microstructural characterization of the specimens, selected from the bottom edge of the cylindrical samples. Porosity levels increased as the amount of nanoparticles in the alloy increased and as stirring time increased.

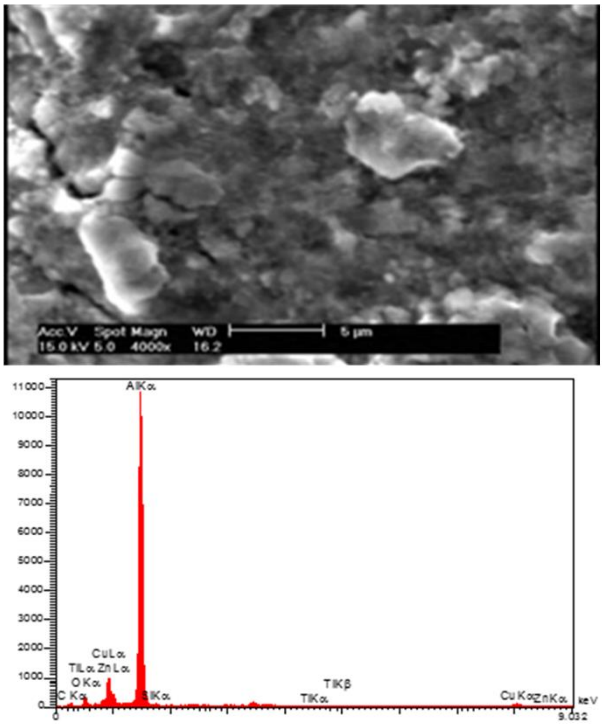

Figure 8. SEM micrographs and EDS analysis of the wear debris:LM2/2 vol% nano-TiC

Hardness, strength, and wear resistance improved with the addition of nano-TiC particles. The maximum hardness and minimum wear rate were recorded for the TiC–Cu reinforced sample stirred for 4 min. Copper strengthened the samples and affected particle dispersion, while porosity was a significant factor affecting the mechanical performance of the materials fabricated at different stirring durations. Hardness and wear resistance of the samples changed longitudinally throughout the cylindrical samples, which was attributed to the local performance of the materials in hardness and wear tests. Variation in wear properties among samples was related different nanoparticle and porosity content in various parts of the cylindrical composites.

References

[1] Davis LC, Andres C, Allison JE. Microstructure and strengthening of metal matrix composites. *Mater Sci Eng A* 1998;249:40–5.

[2] Kok M. Production and mechanical properties of Al2O3 particle-reinforced 2024 aluminum alloy composites. *J Mater Process Technol* 2005;161:381–7.

[3] Miyajima T, Iwai Y. Effects of reinforcements on sliding wear behavior of aluminum matrix composites. *Wear* 2003;255:606–16.

[4] Meyers MA, Mishra A, Benson DJ. Mechanical properties of nanocrystalline materials. *Prog Mater Sci* 2006;51:427–556.

[5] Surappa MK, Prasad SV, Rohatgi PK. Wear and abrasion of cast Al–alumina particle composites. *Wear* 1982;77:295–312.

[6] Razavi-Tousi SS, Yazdani-Rad R, Manafi SA. Effect of volume fraction and particle size of alumina reinforcement on compaction and densification behavior of Al–Al2O3 nanocomposites. *Mater Sci Eng A* 2011; 528:1105–10.

[7] Kang YC, Chan SLI. Tensile properties of nanometric Al2O3 particulate reinforced aluminum matrix composites. *Chem Phys* 2004; 85:438–43.

[8] Yung-Chang K, Lap-Ip CS. Tensile properties of nanometric Al2O3 particulate reinforced aluminum matrix composites. *Mater Chem Phys* 2004;85:438–43.

[9] ajjadi SA, Torabi Parizi M, Ezatpour HR, Sedghi A. Fabrication of A356 composite reinforced with micro and nano particles by a developed compocasting method and study of its properties. *J Alloys Compd* 2012; 511:226–31.

[10] Hashim J, Looney L, Hashmi MSJ. Particle distribution in cast metal matrix composites – Part I. *J Mater Process Technol* 2002;123:251–7.

[11] Mazahery A, Abdizadeh H, Baharvandi HR. Development of high performance A356/nano composites. *Mater Sci Eng A* 2009;518:61–4.

[12] Sokolowski JH, Sun XC, Byczynski G, Northwood DO, Penrod DE, Thomass R, et al. The removal of copper-phase segregation and the subsequent improvement in mechanical properties of cast 319 aluminum alloys by a two-stage solution heat treatment. *J Mater Process Technol* 1995;53:385–92.

[13] Bouvard D. Densification behavior of mixtures of hard and soft powders under pressure*. Powder Technol* 2000;111:231–9.

[14] Nagata S. **Mixing principles and applications**. New York: Wiley; 1975.

[15] Harnby N, Edwards MF, Nienow AW. **Mixing in the process industries.** 2nd ed. Oxford: Butterworth-Heinemann; 1997.

[16] Ansary Yar A, Montazerian M, Abdizadeh H, Baharvandi HR. Microstructure and mechanical properties of aluminum alloy matrix composite reinforced with nano-particle MgO. *J Alloys Compd* 2009;484:400–4.

[17] Abdizadeh H, Baharvandi HR, Shirvani Moghaddam K. Comparing the effect of processing temperature on microstructure and mechanical behavior of (ZrSiO4 or TiB2)/aluminum composites. *Mater Sci Eng* 2008;498:53–8.

[18] Reed-Hill RE, Abbaschian R. **Physical metallurgy principles.** 3rd ed. Boston: PWS; 1994.

[19] Geiger AL, Walker JA. The processing and properties of discontinuously reinforced aluminum composites. *J Met* 1991;43:8–15.

[20] Miyajima T, Iwai Y. Effects of reinforcements on sliding wear behavior of aluminum matrix composites. *Wear* 2003; 255:606.

[21] Kok M. Abrasive wear of Al2O3 particle reinforced 2024 aluminum alloy composite fabricated by vortex method. *Compos: Part A* 2006;37:457–64.

[22] Kok M, Ozdin K. Wear resistance of aluminum alloy and its composites reinforced by Al2O3 particles. *J Mater Process Technol* 2007;183:301–9.

[23] Sjolander E, Seifeddine S. The heat treatment of Al–Si–Cu–Mg casting alloys. *J Mater Process Technol* 2010;210:1249–59.

[24] Leon CA, Mendeza-Suarez G, Drew RAL. Wettability and spreading kinetics of molten aluminum on copper-coated ceramics. *J Mater Sci* 2006;41:5081–7.

[25] Li Z, Samuel AM, Samuel FH. Effect of alloying elements on the segregation and dissolution of CuAl2 phase in Al–Si–Cu 319 alloys. *J Mater Sci* 2003; 38:1203–18.